Strong electromagnetic fields and flows in relativistic heavy-ion collisions

Viacheslav Toneev (JINR)

In collaboration with
Wolfgang Cassing (Giessen)
Vadim Voronyuk (JINR)

Brazil-JINR Forum
Dubna, June 15-19, 2015

From hadrons to partons

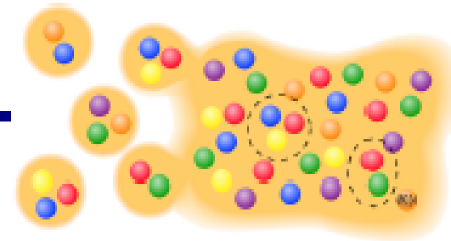

In order to study the phase transition from hadronic to partonic matter – Quark-Gluon-Plasma – we need a consistent non-equilibrium (transport) model with

- explicit parton-parton interactions (i.e. between quarks and gluons) beyond strings!
- explicit phase transition from hadronic to partonic degrees of freedom
- lQCD EoS for partonic phase

Transport theory: off-shell Kadanoff-Baym equations for the Green-functions $S^{<}_{h}(x,p)$ in phase-space representation for the partonic and hadronic phase

⇨ **Parton-Hadron-String-Dynamics (PHSD)**

W. Cassing, E. Bratkovskaya, PRC 78 (2008) 034919; NPA 831 (2009) 215; W. Cassing, EPJ ST 168 (2009) 3

QGP phase described by

Dynamical QuasiParticle Model (DQPM)

A. Peshier, W. Cassing, PRL 94 (2005) 172301; Cassing, NPA 791 (2007) 365: NPA 793 (2007)

The Dynamical QuasiParticle Model (DQPM)

Basic idea: Interacting quasiparticles

- massive quarks and gluons (g, q, q_{bar}) with spectral functions :

$$\boxed{\rho(\omega) = \frac{\gamma}{\mathrm{E}}\left(\frac{1}{(\omega-\mathrm{E})^2+\gamma^2} - \frac{1}{(\omega+\mathrm{E})^2+\gamma^2}\right)}$$

$$E^2 = p^2 + M^2 - \gamma^2$$

▪ quarks

▪ gluons:

A. Peshier, PRD 70 (2004) 034016

mass:

$$m^2(T) = \frac{N_c^2-1}{8N_c} g^2 \left(T^2 + \frac{\mu_q^2}{\pi^2}\right)$$

$$\mathrm{M}^2(\mathrm{T}) = \frac{\mathrm{g}^2}{6}\left((\mathrm{N_c} + \frac{1}{2}\mathrm{N_f})\,\mathrm{T}^2 + \frac{\mathrm{N_c}}{2}\sum_q \frac{\mu_q^2}{\pi^2}\right)$$

$N_c = 3$, $N_f = 3$

width:

$$\gamma_q(\mathrm{T}) = \frac{\mathrm{N_c^2}-1}{2\mathrm{N_c}} \frac{\mathrm{g^2 T}}{4\pi} \ln\frac{\mathrm{c}}{\mathrm{g}^2}$$

$$\gamma_g(\mathrm{T}) = \mathrm{N_c}\frac{\mathrm{g^2 T}}{4\pi} \ln\frac{\mathrm{c}}{\mathrm{g}^2}$$

running coupling: $\alpha_S(T) = g^2(T)/(4\pi)$

$$\mathrm{g}^2(\mathrm{T/T_c}) = \frac{48\pi^2}{(11\mathrm{N_c} - 2\mathrm{N_f})\ln(\lambda^2(\mathrm{T/T_c} - \mathrm{T_s/T_c})^2}$$

➢ fit to lattice (lQCD) results (e.g. entropy density)

with 3 parameters: $T_s/T_c=0.46$; $c=28.8$; $\lambda=2.42$

➔ quasiparticle properties (mass, width)

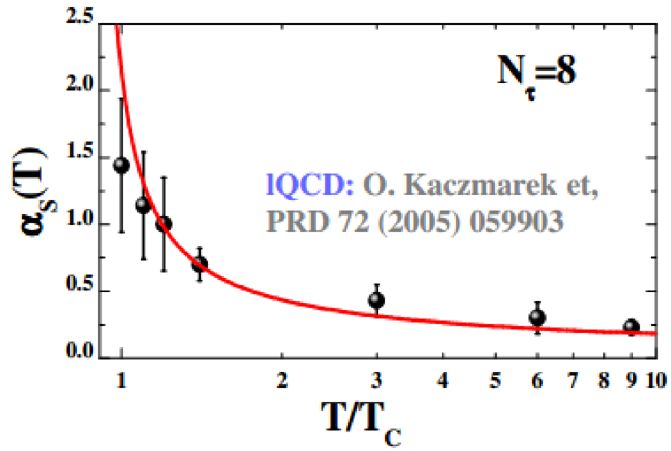

DQPM: Peshier, Cassing, PRL 94 (2005) 172301;
Cassing, NPA 791 (2007) 365: NPA 793 (2007)

The Dynamical QuasiParticle Model (DQPM)

➔ **Quasiparticle properties:**

- **large width and mass for gluons and quarks**

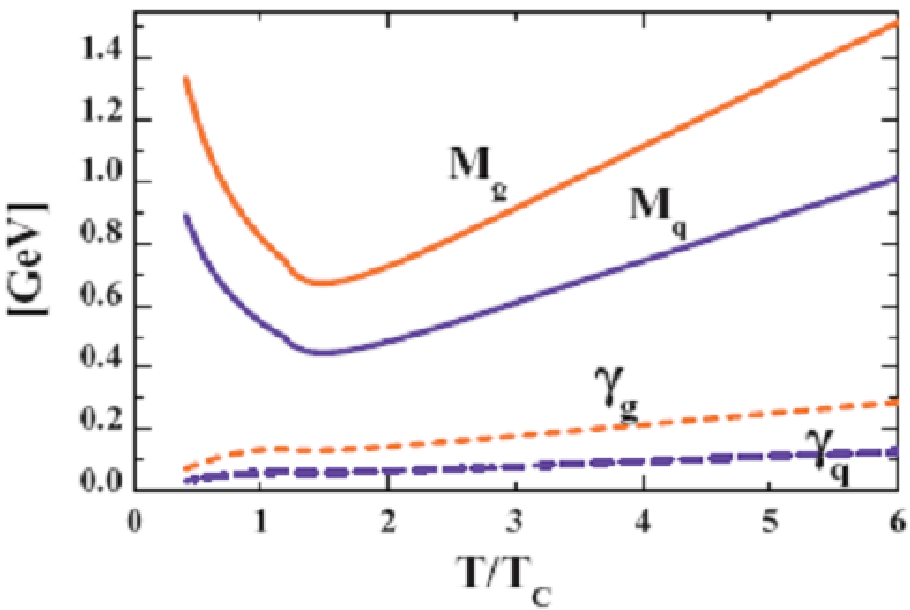

➔ **Broad spectral function :**

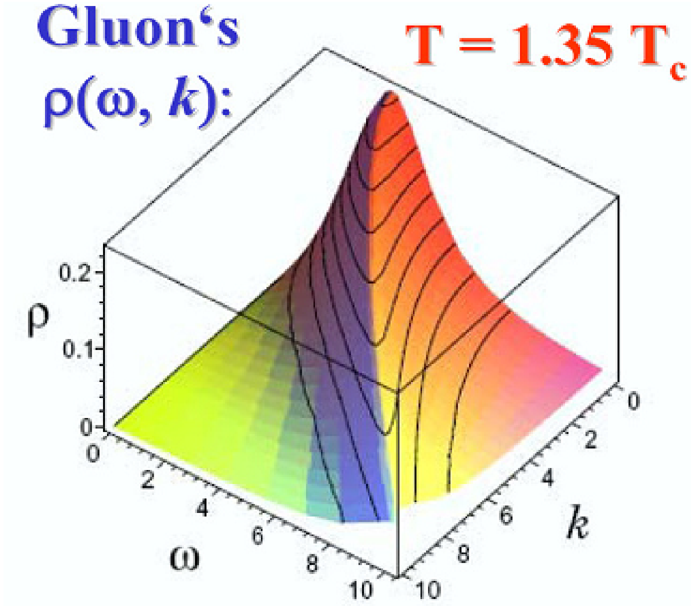

- **DQPM matches well lattice QCD**
- **DQPM provides mean-fields (1PI) for gluons and quarks as well as effective 2-body interactions (2PI)**
- **DQPM gives transition rates for the formation of hadrons ➔ PHSD**

Peshier, Cassing, PRL 94 (2005) 172301; Cassing, NPA 791 (2007) 365: NPA 793 (2007)

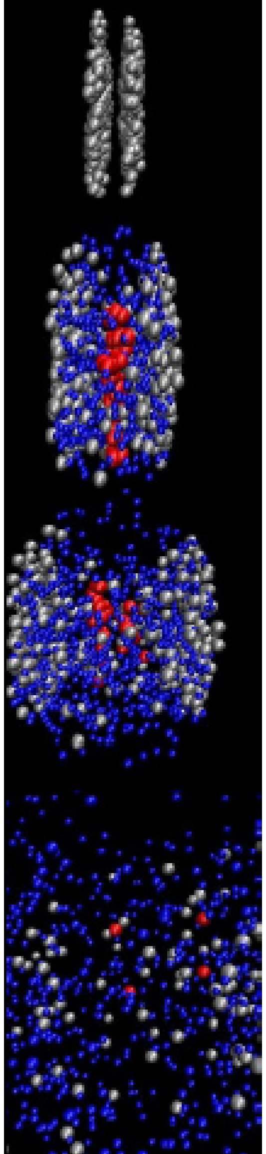

PHSD - basic concept

Initial A+A collisions – HSD: string formation and decay to pre-hadrons

Fragmentation of pre-hadrons into quarks: using the quark spectral functions from the Dynamical QuasiParticle Model (DQPM) - approximation to QCD

Partonic phase: quarks and gluons (= ‚dynamical quasiparticles') with off-shell spectral functions (width, mass) defined by the DQPM

- ❑ elastic and inelastic parton-parton interactions:

using the effective cross sections from the DQPM

- ✓ q + qbar (flavor neutral) <=> gluon (colored)
- ✓ gluon + gluon <=> gluon (possible due to large spectral width)
- ✓ q + qbar (color neutral) <=> hadron resonances

- ❑ self-generated mean-field potential for quarks and gluons !

Hadronization: based on DQPM - massive, off-shell quarks and gluons with broad spectral functions hadronize to off-shell mesons and baryons:
gluons → q + qbar; q + qbar → meson (or string);
q + q +q → baryon (or string) (strings act as ‚doorway states' for hadrons)

Hadronic phase: hadron-string interactions – off-shell HSD

W. Cassing, E. Bratkovskaya, PRC 78 (2008) 034919;
NPA831 (2009) 215; EPJ ST 168 (2009) 3; NPA856 (2011) 162.

PHSD: snapshot in the reaction plane

t = 3 fm/c

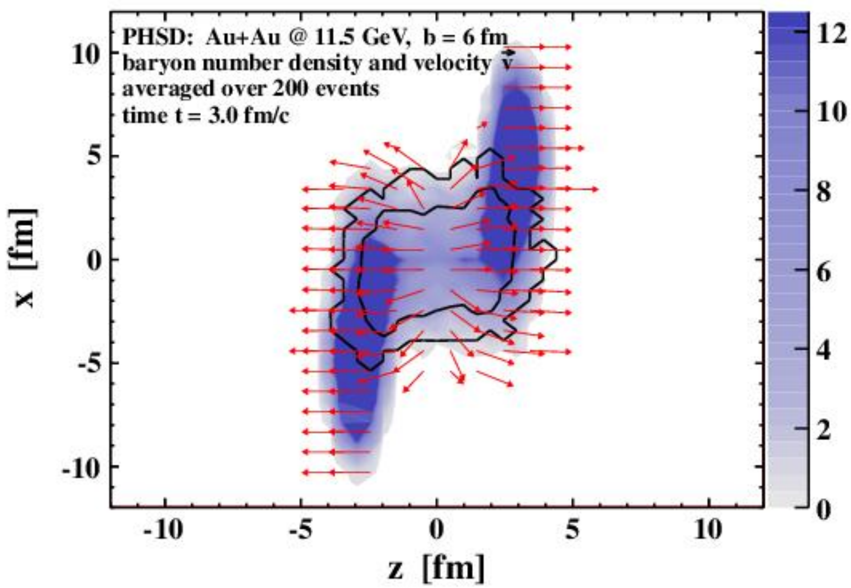

t = 6 fm/c

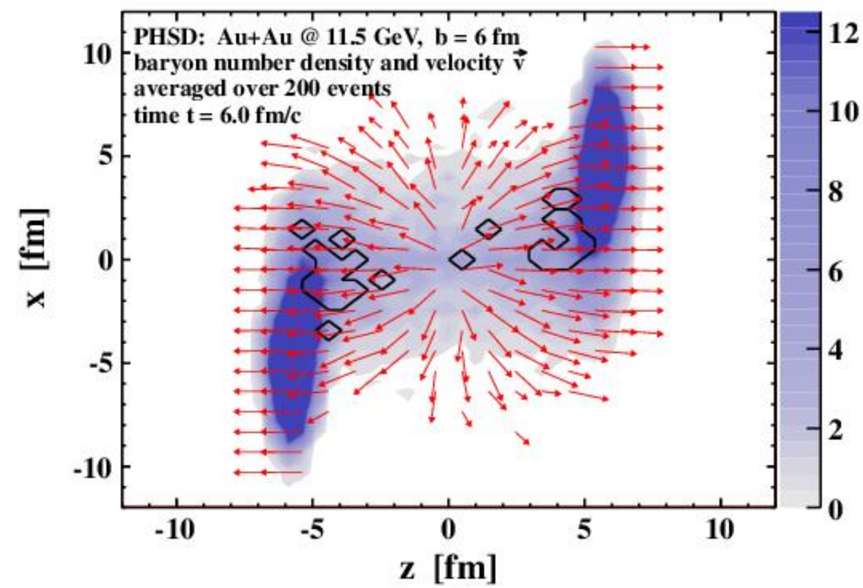

- Color scale: baryon number density
- Black levels: parton density 0.6 and 0.01 fm^{-3}
- Red arrows: local velocity of baryon matter

(P)HSD: multiplicities at midrapidity

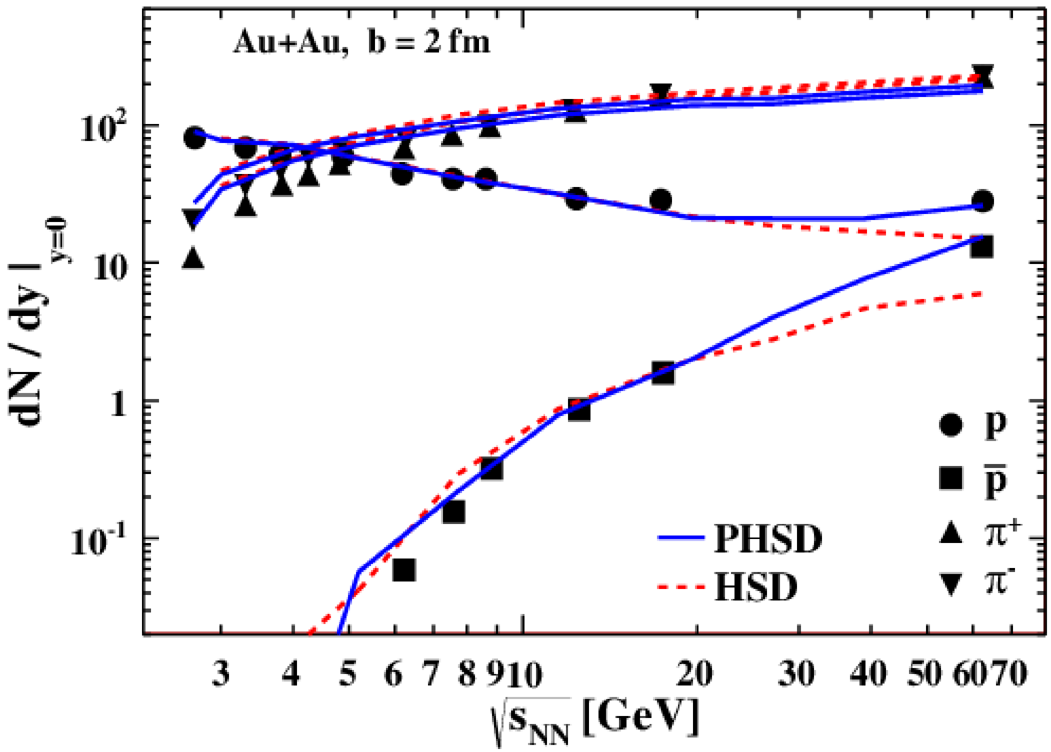

- Transport approach works reasonably good
- Deviations from the data appear for HSD at √s > 20 GeV

A. Andronic, P. Braun-Munzinger and J. Stachel, Nucl. Phys. **A772,** 167 (2006)

Excitation function of elliptic flow

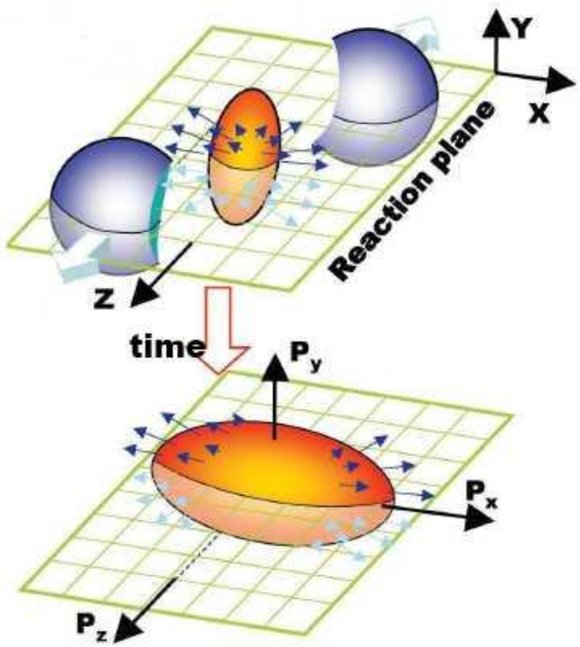

$$\frac{dN}{d\varphi} \propto \left(1 + 2\sum_{n=1}^{+\infty} v_n \cos[n(\varphi - \psi_n)]\right)$$

$$v_n = \langle \cos n(\varphi - \psi_n) \rangle, \quad n = 1,2,3..,$$

$$v_1 = \left\langle \frac{p_x}{p_T} \right\rangle, \quad v_2 = \left\langle \frac{p_x^2 - p_y^2}{p_x^2 + p_y^2} \right\rangle$$

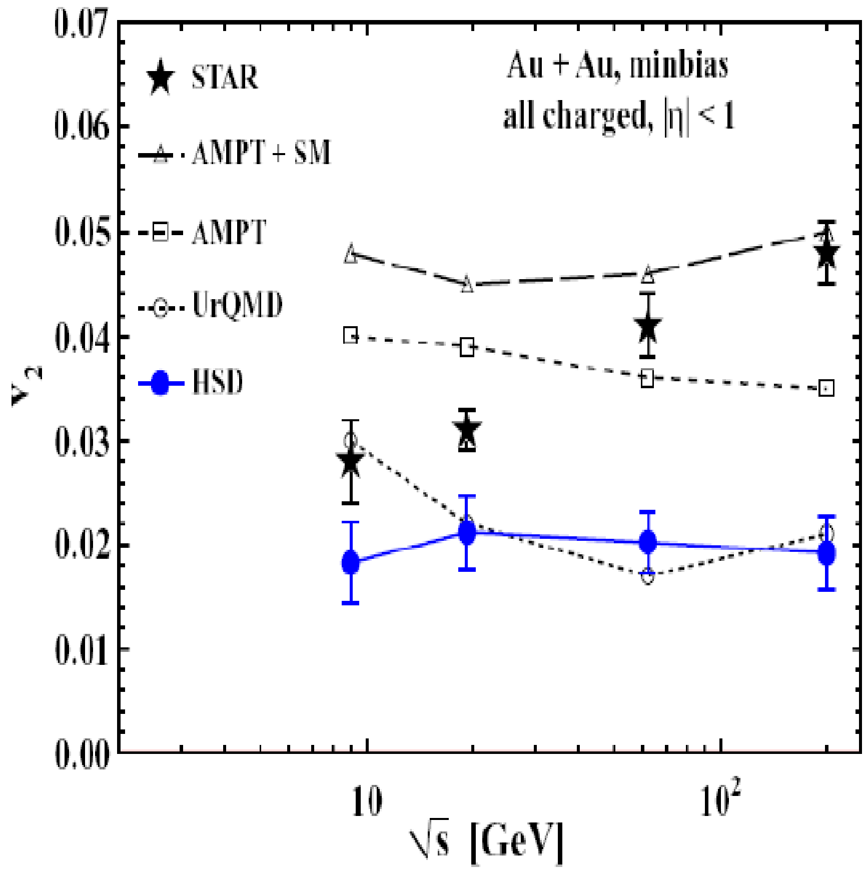

is not described by hadron-string or purely partonic models !

Elliptic flow from PHSD vs. STAR/PHENIX

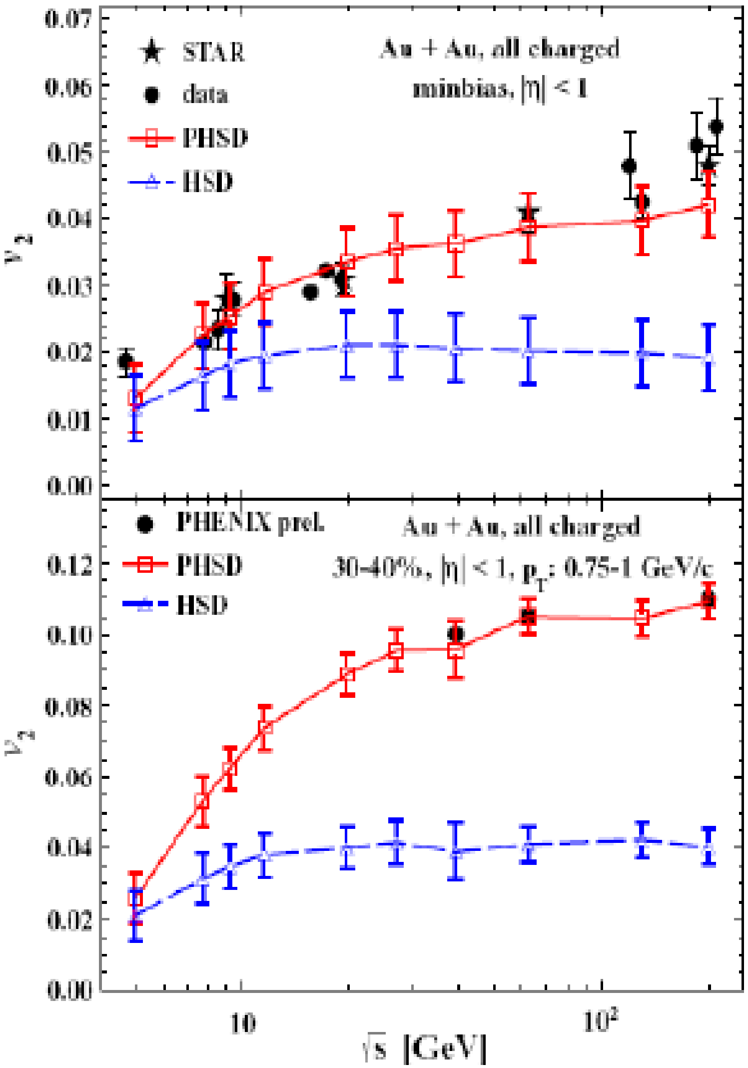

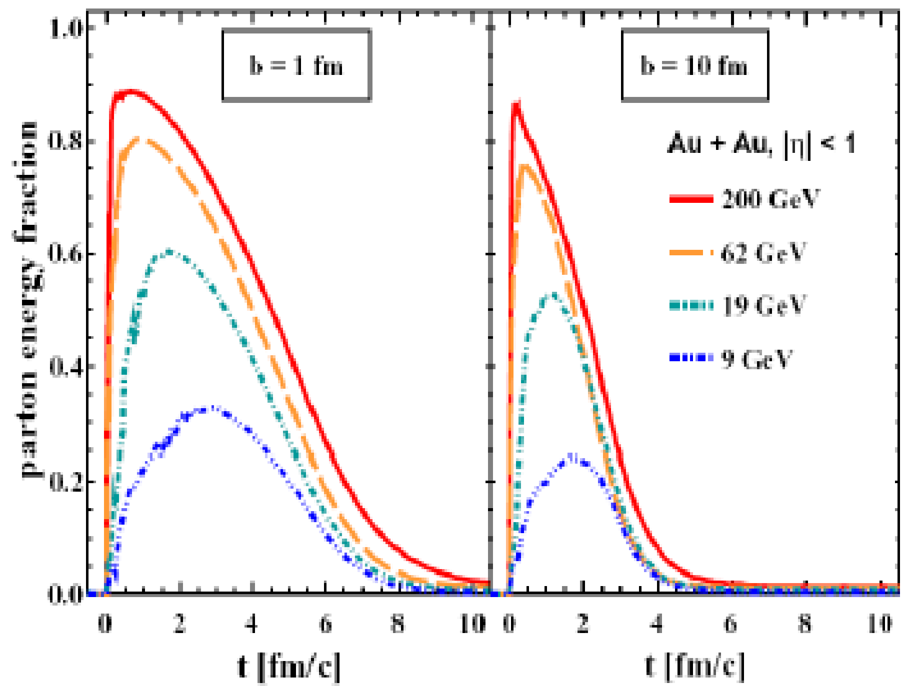

is reasonably described by PHSD due to an increasing fraction of partonic degrees-of-freedom !

V.Konchakovski et al. PR C65, 011902 (2012)

Transport model with electromagnetic field

Generalized on-shell transport equations in the presence of electromagnetic fields can be obtained formally by the substitution:

$$\{\frac{\partial}{\partial t} + \left(\frac{\vec{p}}{p_0} + \vec{\nabla}_{\vec{p}}\, U\right)\vec{\nabla}_{\vec{r}} - \left(\vec{\nabla}_{\vec{r}}\, U - e\vec{E} - e\vec{v}\times\vec{B}\right)\vec{\nabla}_{\vec{p}}\,\}\, f(\vec{r},\vec{p},t) = I_{coll}(f, f_1, ... f_N)$$

$$\dot{\vec{r}} \to \frac{\vec{p}}{p_0} + \vec{\nabla}_p U\ ,$$

$$\dot{\vec{p}} \to -\vec{\nabla}_r U + e\vec{E} + e\vec{v}\times\vec{B}$$

$$U \sim Re(\Sigma^{ret})/2p_0$$

A general solution of the wave equations is as follows

$$div\ \mathbf{B} = 0 \qquad div\ \mathbf{E} = 4\pi\rho$$

$$rot\ \mathbf{E} = -\frac{\partial \mathbf{B}}{\partial t} \qquad rot\ \mathbf{B} = \frac{\partial \mathbf{E}}{\partial t} + \frac{4\pi}{c}\mathbf{j}$$

$$\vec{A}(\vec{r},t) = \frac{1}{4\pi}\int \frac{\vec{j}(\vec{r'},t')\ \delta(t-t'-|\vec{r}-\vec{r'}|/c)}{|\vec{r}-\vec{r'}|}\, d^3r'dt'$$

$$\Phi(\vec{r},t) = \frac{1}{4\pi}\int \frac{\rho(\vec{r'},t')\ \delta(t-t'-|\vec{r}-\vec{r'}|/c)}{|\vec{r}-\vec{r'}|}\, d^3r'dt'$$

$$\begin{cases} \vec{B} = \vec{\nabla}\times\vec{A} \\ \vec{E} = -\vec{\nabla}\Phi - \dfrac{\partial\vec{A}}{\partial t} \end{cases}$$

For point-like particles $\rho(\vec{r},t) = e\ \delta(\vec{r}-\vec{r}(t));\quad \vec{j}(\vec{r},t) = e\ \vec{v}(t)\ \delta(\vec{r}-\vec{r}(t))$

$$e\mathbf{B}(t,\mathbf{r}) = \frac{e^2}{4\pi}\sum_n Z_n(\mathbf{R}_n)\frac{1-v_n^2}{[R_n^2-(\mathbf{R}_n\times\mathbf{v}_n)^2]^{3/2}}\mathbf{v}_n\times\mathbf{R}_n$$

$$e\mathbf{E}(t,\mathbf{r}) = \frac{e^2}{4\pi}\sum_n Z_n(\mathbf{R}_n)\frac{1-v_n^2}{[R_n^2-(\mathbf{R}_n\times\mathbf{v}_n)^2]^{3/2}}\mathbf{R}_n,$$

Liénard-Wiechert potential

b $\to 0$	$e\mathbf{B}, e\mathbf{E} \to 0$
v $\to 0$	$e\mathbf{B} \to 0,\ e\mathbf{E} \neq 0$
high energy	$e\mathbf{B}$ transverse
symmetry	only $eB_y \neq 0$

Magnetic field evolution

For a single moving charge (HSD calculation result)

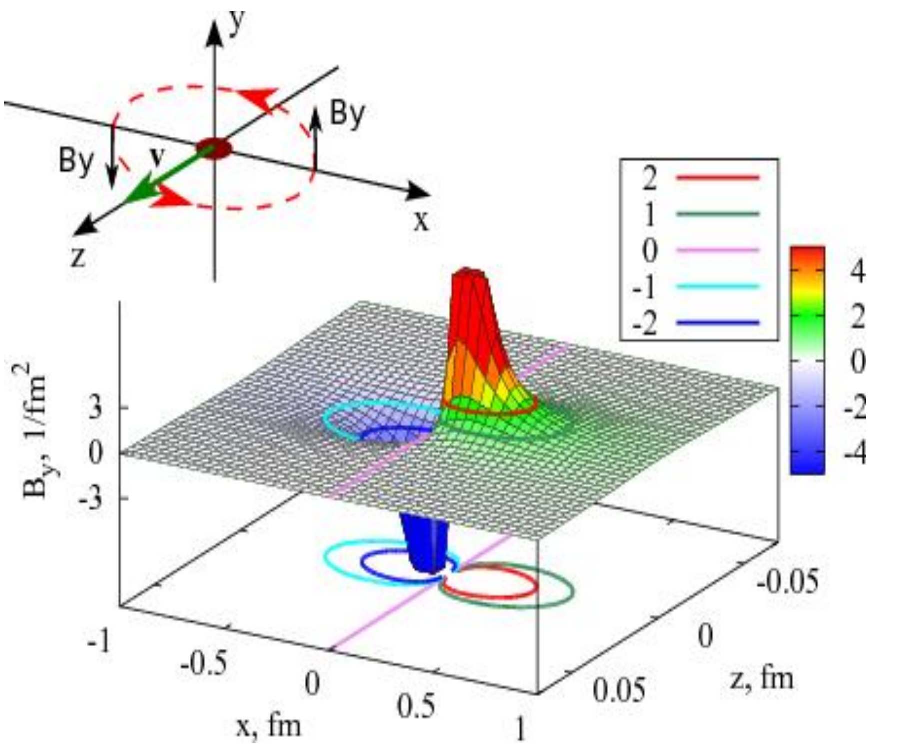

For two-nuclei collisions, artist's view: arXiv:1109.5849

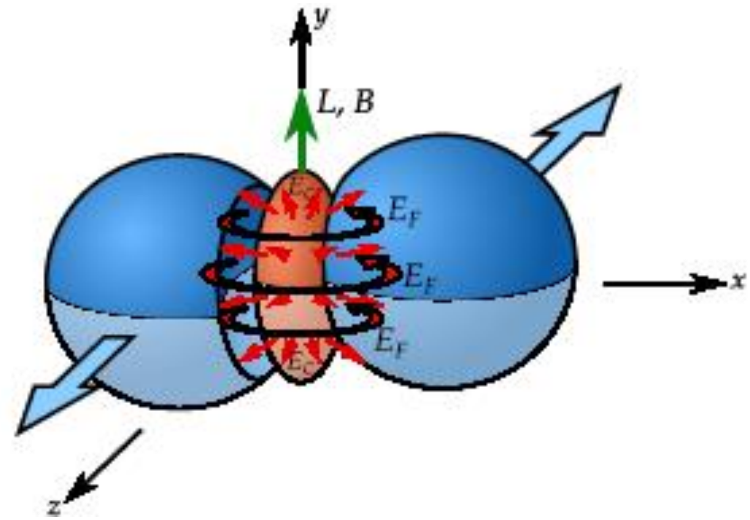

Time evolution of magnetic field

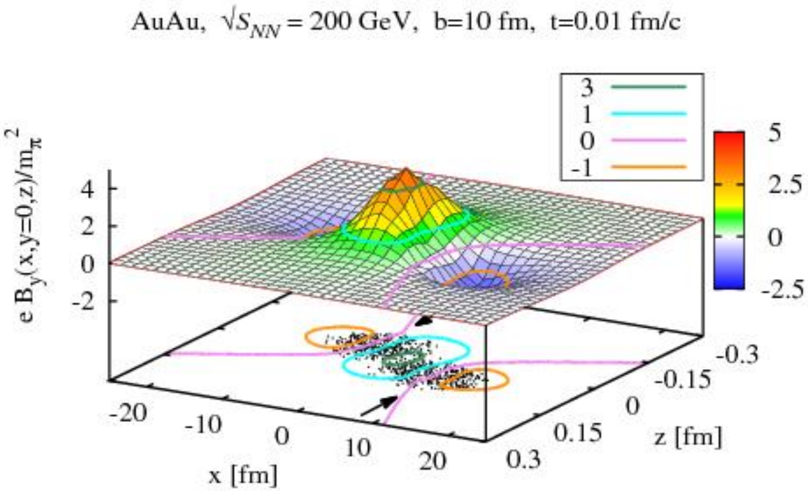

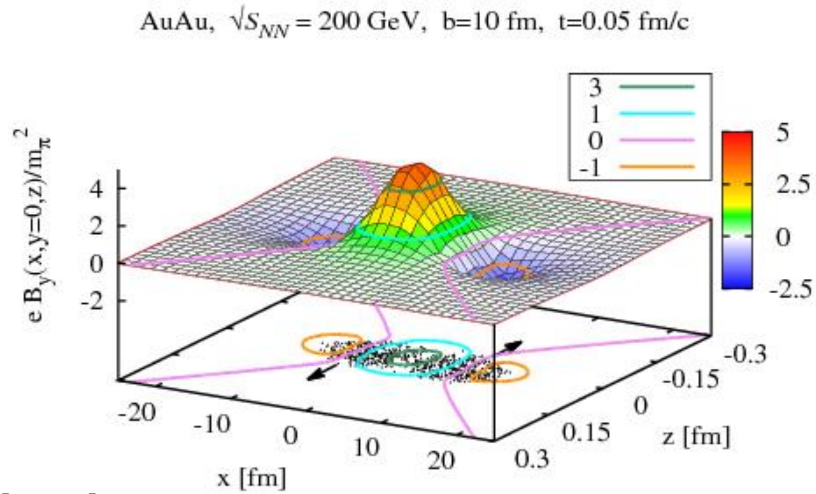

Au+Au(200)
b=10 fm

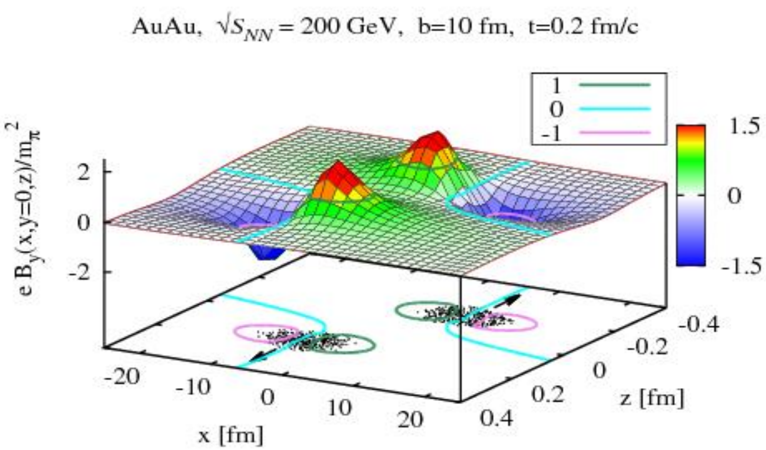

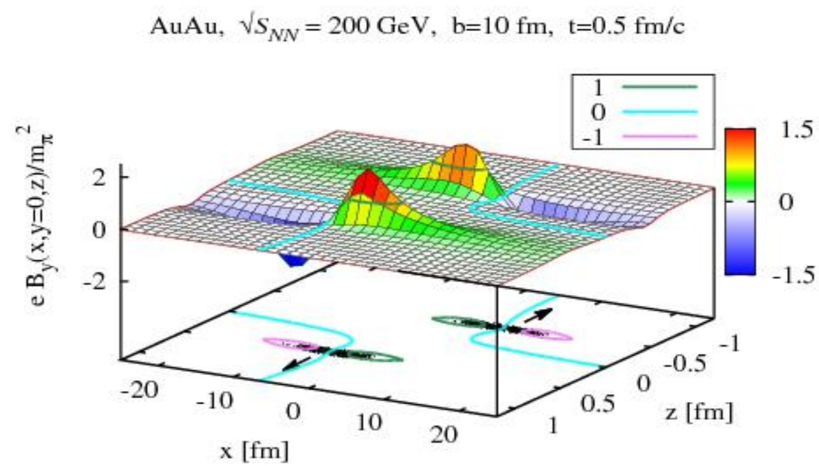

V.Voronyuk, V.T. et al., Phys. Rev. **C84**, 035202 (2011)

Time dependence of eB_y

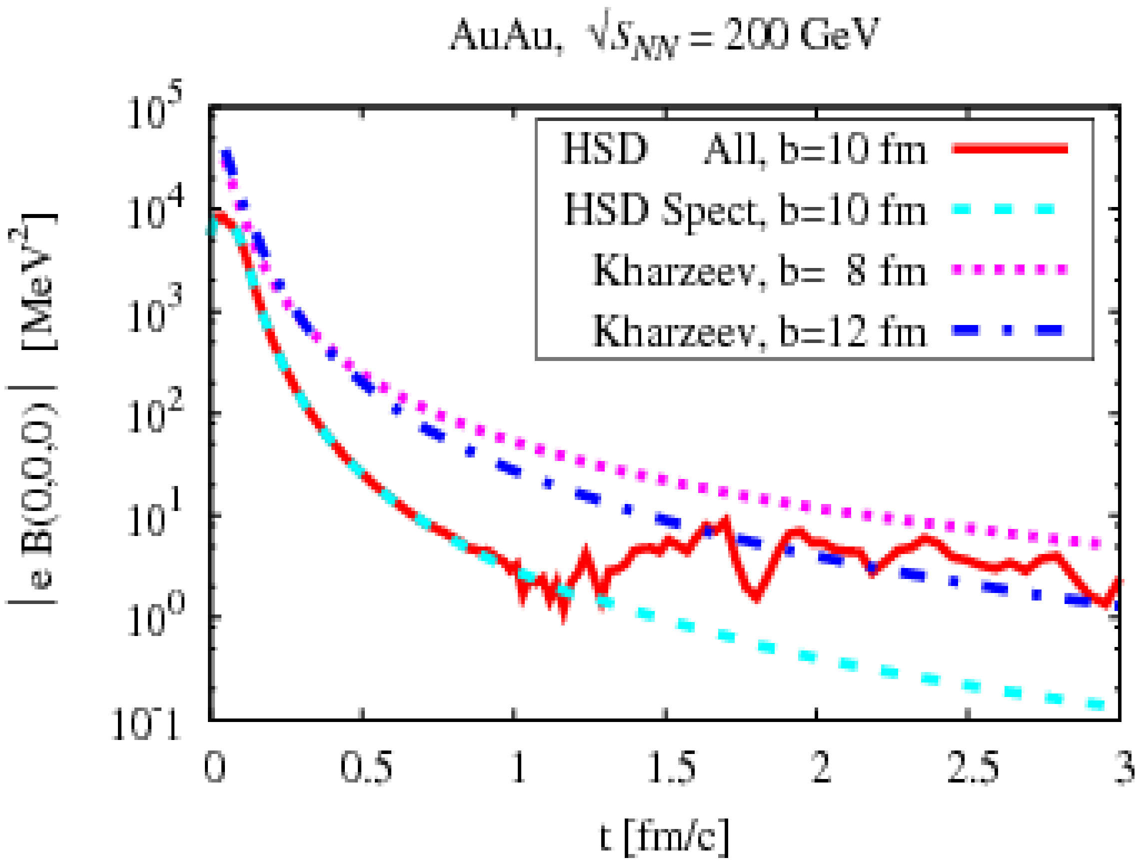

D.E. Kharzeev et al., Nucl. Phys. **A803**, 227 (2008**)**
Collision of two infinitely thin layers (pancake-like)

V. Voronyuk, V. T. et al., PR **C84**, 035202 (2011)

Until t~1 fm/c the induced magnetic field is defined by spectators only. Maximal magnetic field is reached during nuclear overlapping time Δt~0.2 fm/c, then the field goes down exponentially.

Beam energy dependence of eB_y

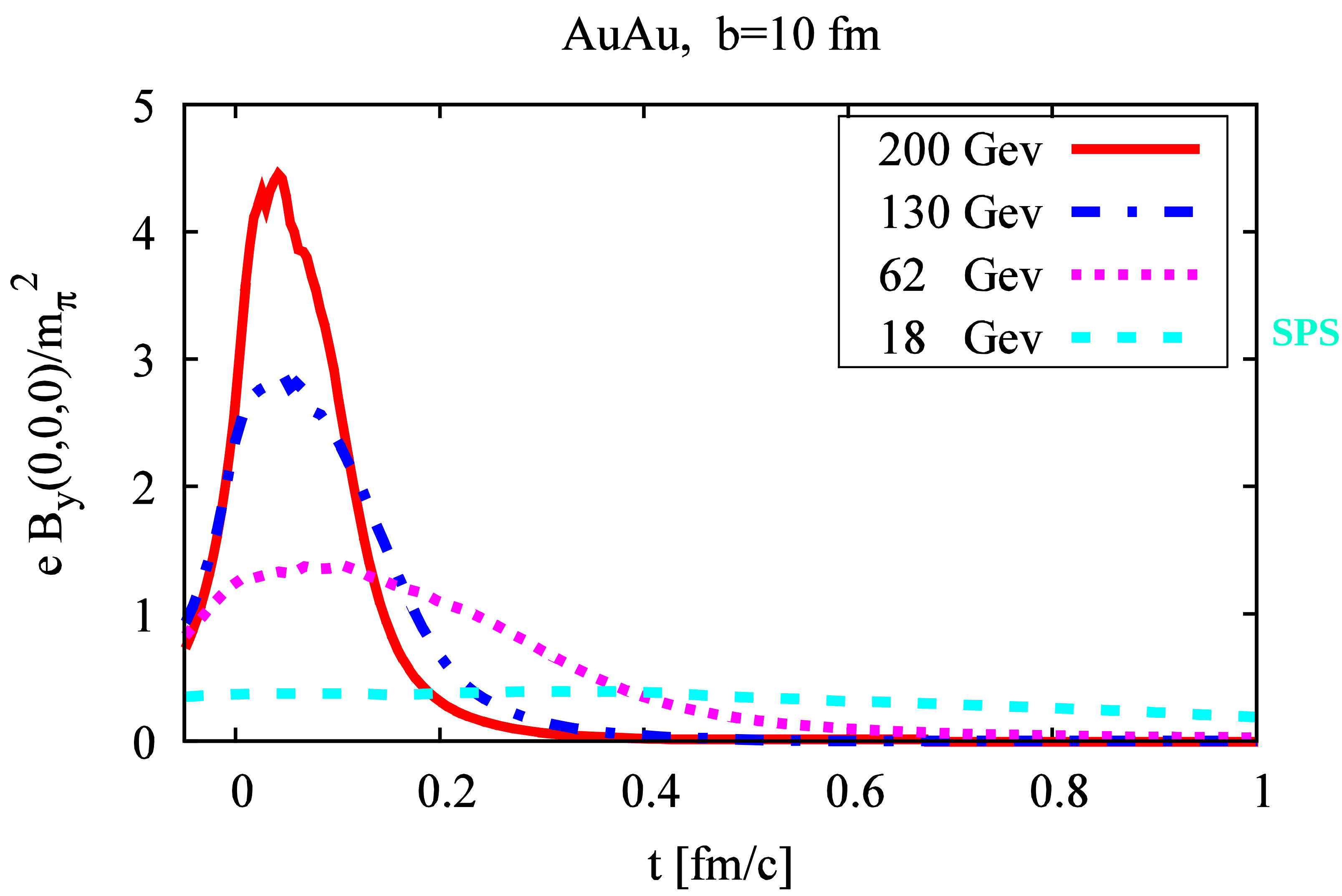

Comparison of magnetic fields

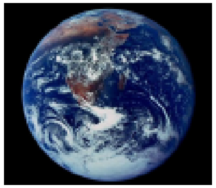

The Earths magnetic field	0.6 Gauss
A common, hand-held magnet	100 Gauss
The strongest steady magnetic fields achieved so far in the laboratory	4.5 x 10^5 Gauss
The strongest man-made fields ever achieved, if only briefly	10^7 Gauss
Typical surface, polar magnetic fields of radio pulsars	10^{13} Gauss
Surface field of Magnetars	10^{15} Gauss

http://solomon.as.utexas.edu/~duncan/magnetar.html

several times 10^{18} G
Phys. Rev. C 89, 045805 (2014)

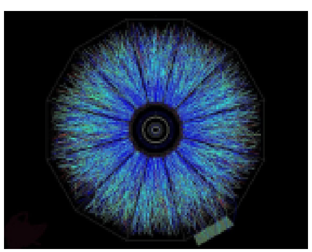

At BNL we beat them all!

Off central Gold-Gold Collisions at 100 GeV per nucleon

$$e\,B(\tau=0.2\,\mathrm{fm}) \;=\; 10^3 \sim 10^4\ \mathrm{MeV}^2 \sim 10^{17}\,\mathrm{Gauss}$$

beam energy	peak value of $eB_y/(m_\pi^2)$
9 GeV (NICA)	~ 0.2
200 GeV (RHIC)	~ 4
2.76 TeV (LHC)	~ 10

$m_\pi^2 \approx 10^{18}$Gauss

Electric field evolution

Electric field of a single moving charge has a "hedgehog" shape

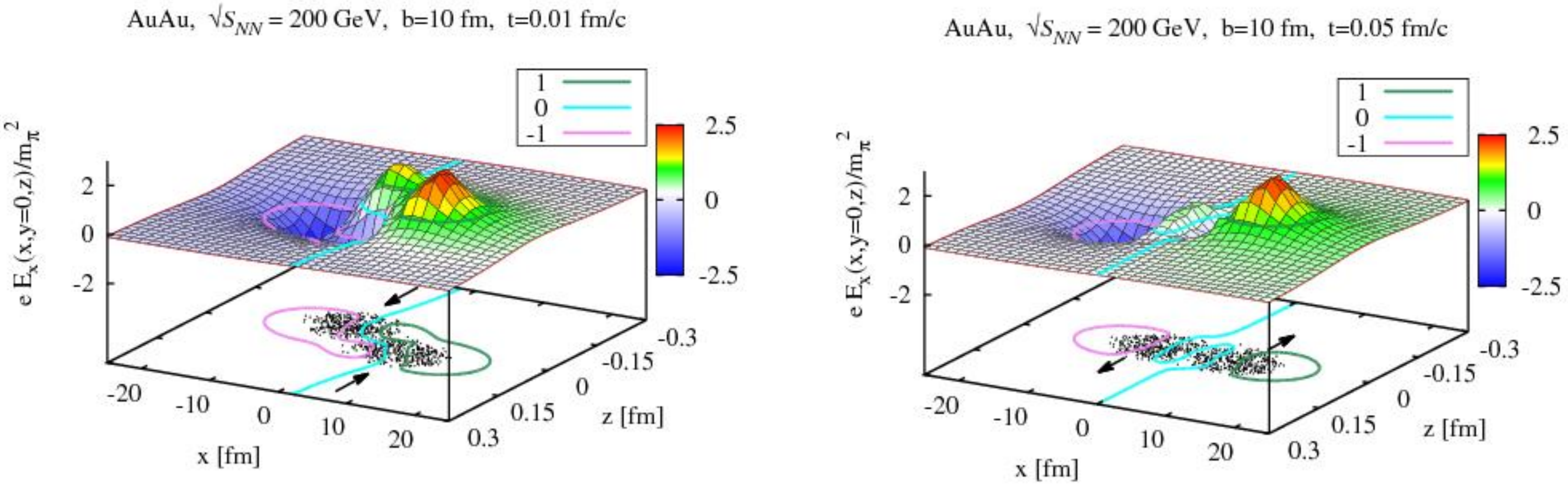

V.Voronyuk, V.T. et al., Phys. Rev. **C84**, 035202 (2011)

Observable

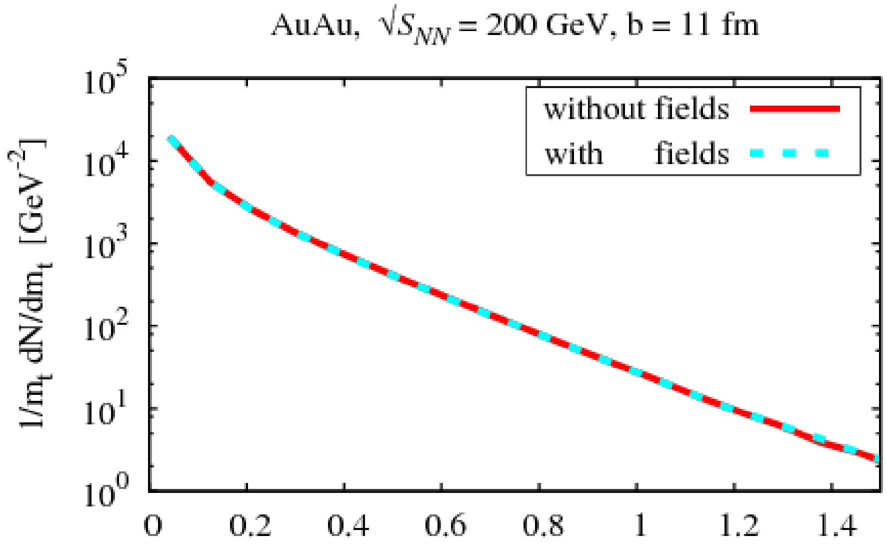

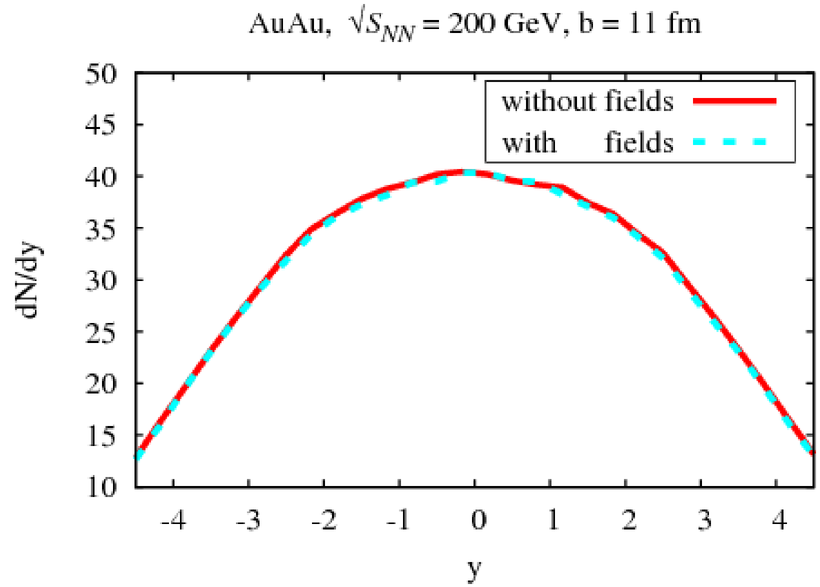

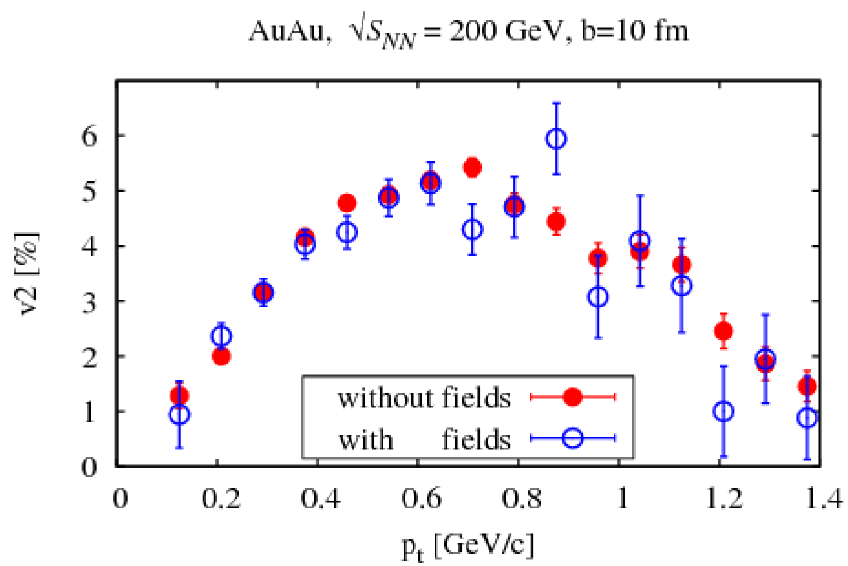

No electromagnetic field effects on global observable in symmetric nuclear collisions !

V.Voronyuk, V.T. et al., Phys. Rev. **C84**, 035202 (2011)

Compensation of electric and magnetic forces

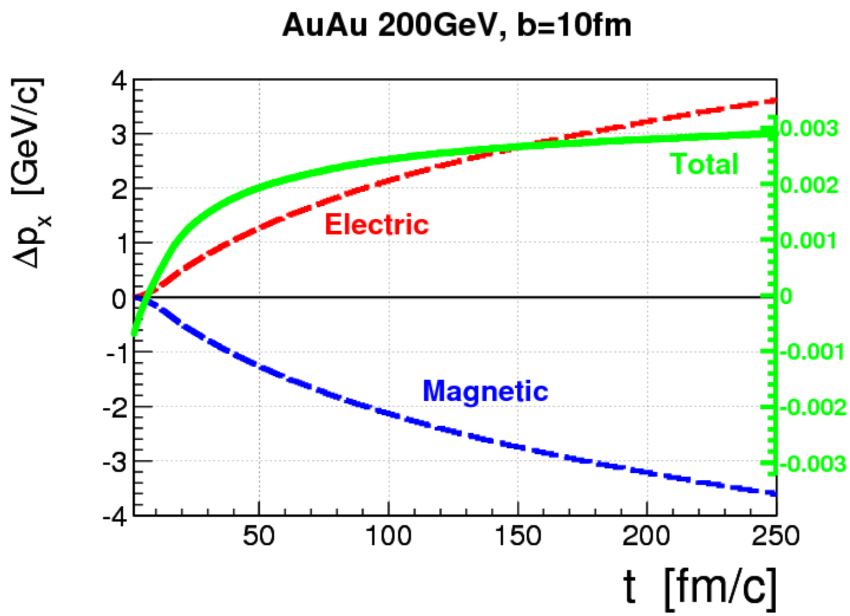

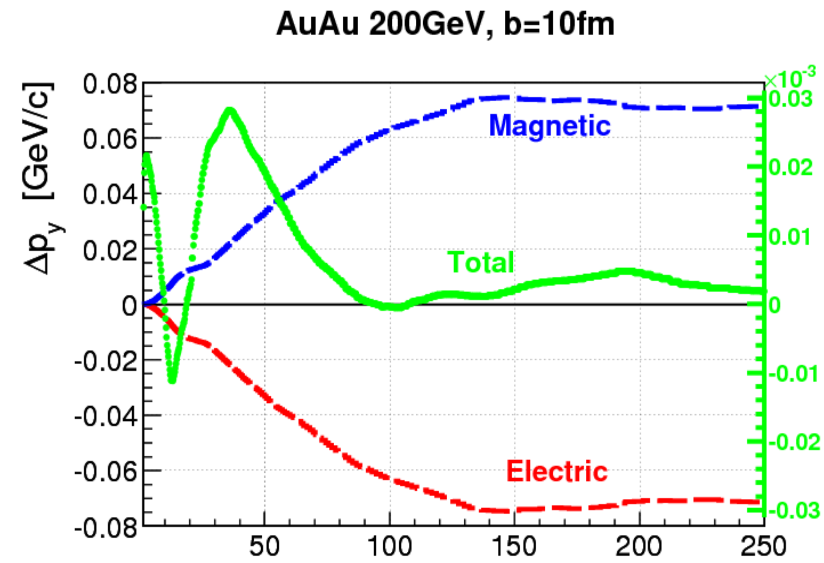

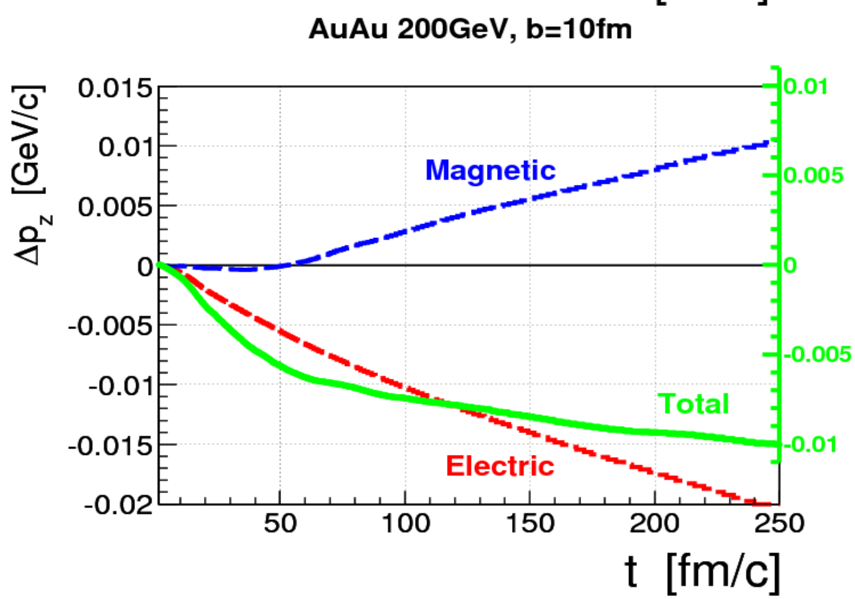

$$\vec{p} \to eE + e\vec{v} \times B$$

$$\Delta\vec{p} = \sum_i \langle\, \delta\vec{p}\, \rangle_i \qquad for \quad p_z > 0$$

Transverse momentum increments Δp due to electric and magnetic fields compensate each other !

$$eE = -e\frac{\partial A}{\partial t} \sim -e\frac{\partial A}{\partial x}\frac{dx}{dt} \sim -eBv$$

CME: Charge separation: CP violation signal

A remarkable property of gauge theories is the existance of nontrivial topological configurations of gauge fields. Gauge field transitions with changing the topological charge involve configurations which may violate $\mathcal{P}$ and $\mathcal{CP}$ invariance of strong interactions.

Fermions can interact with a gauge field configurations, transforming left- into right-handed quarks and vice-versa via the axial chiral anomaly and thus resulting in generated asymmetry between left- and right-handed fermions. In this states a balance between left-handed and right-handed chiral quarks is destroyed.

In the presence of inbalanced chirality a magnetic field induces a chiral electric current along the the magnetic field **(CME)**.

D.Kharzeev et al., NP **A803,** 227 (2008);

Ann.Phys**. 325,** 205 (2010); PR **D78,** 074033 (2008)

Angular correlation wrt. reaction plane

$$\langle \cos(\psi_\alpha + \psi_\beta - 2\Psi_{RP}) \rangle$$

S.Voloshin, PR **C79**, 057901 (2004)

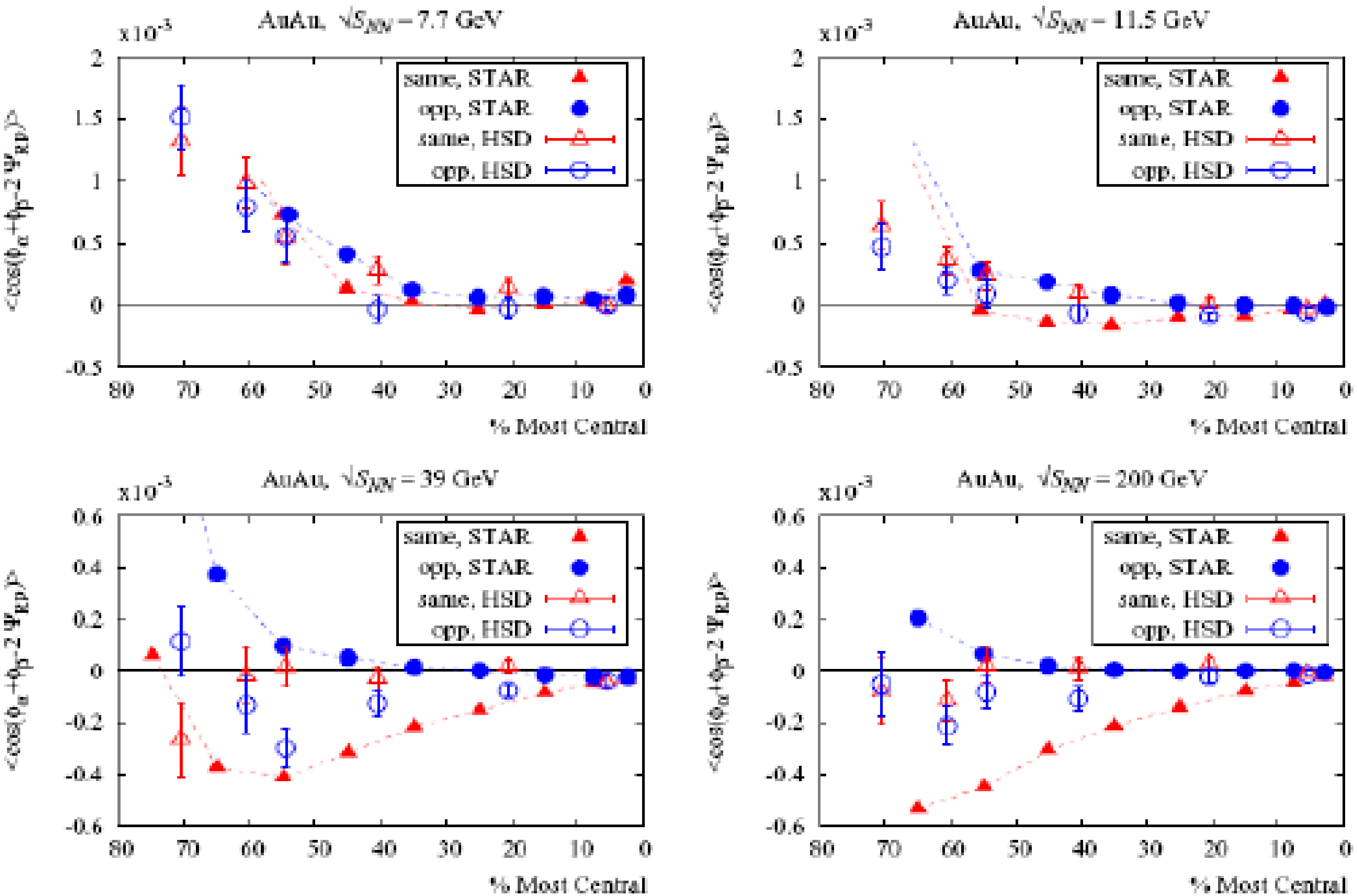

Angular correlation is of hadronic origin **up to** √s=11 GeV !

Electric field E_x in the transverse plane

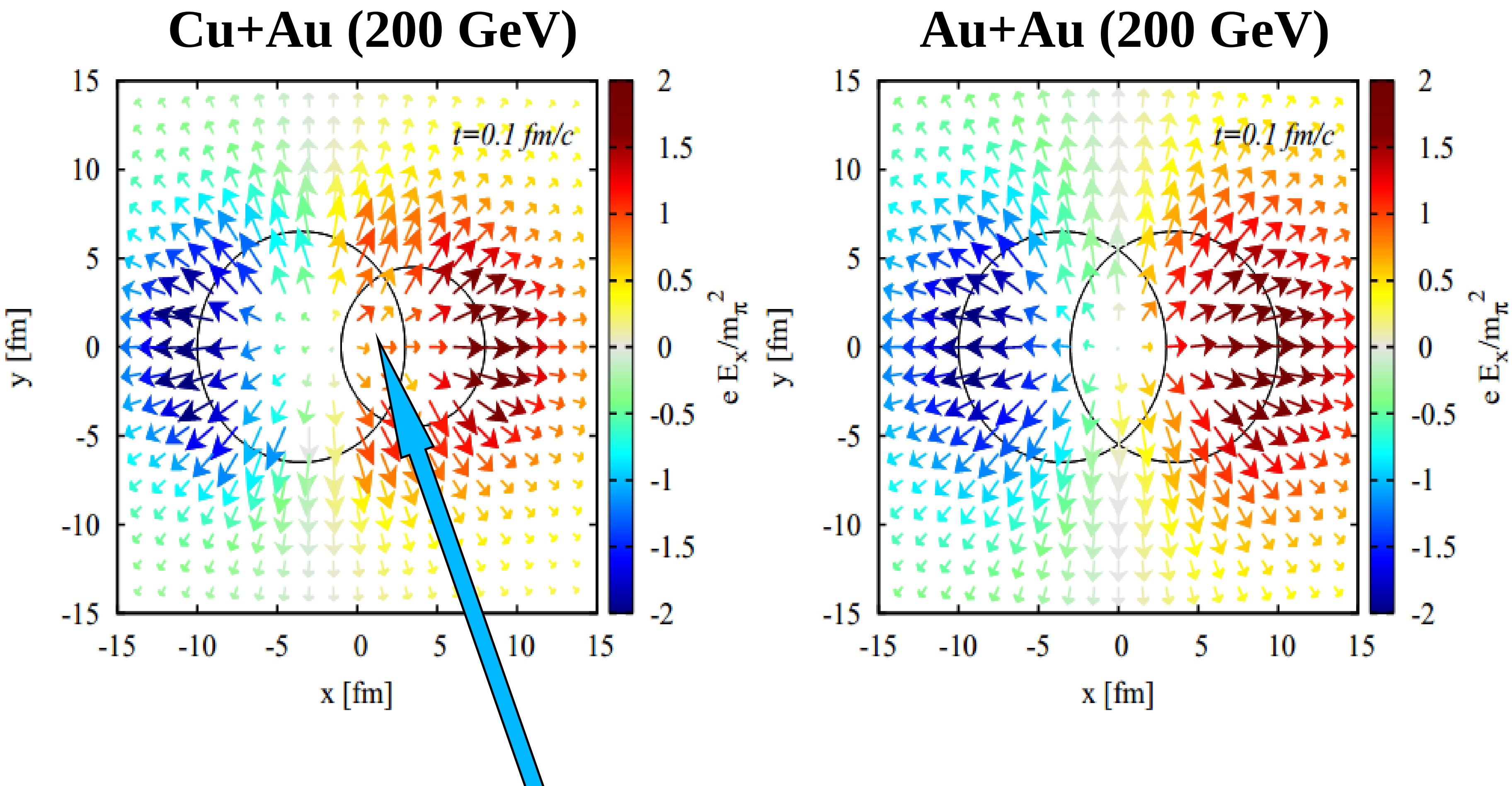

In the overlapping region of asymmetric peripheral collisions a finite electric current appears to be directed from the heavy nuclei to light one.

Charge-dependent v_1 distributions at RHIC

Cu+Au (200 GeV)

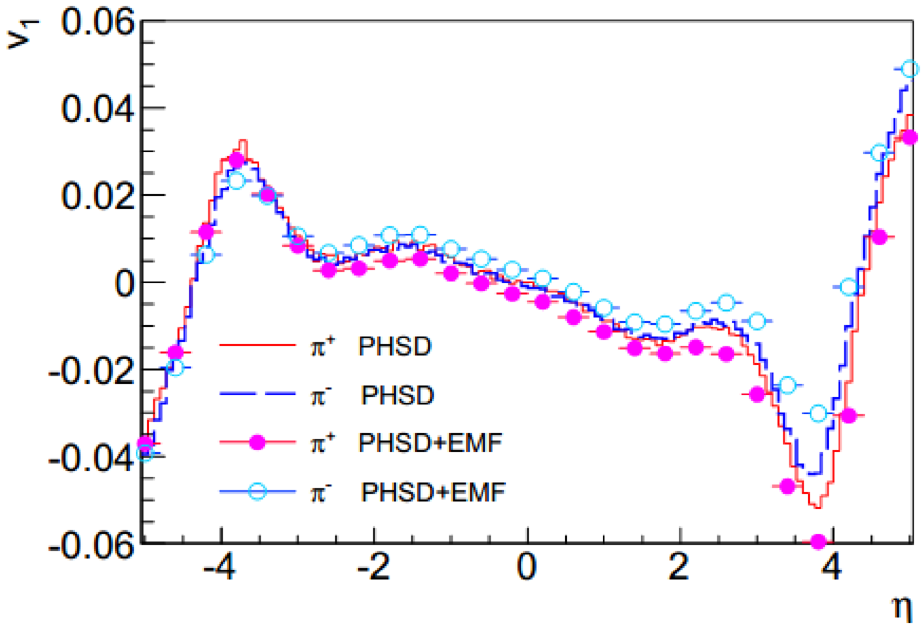

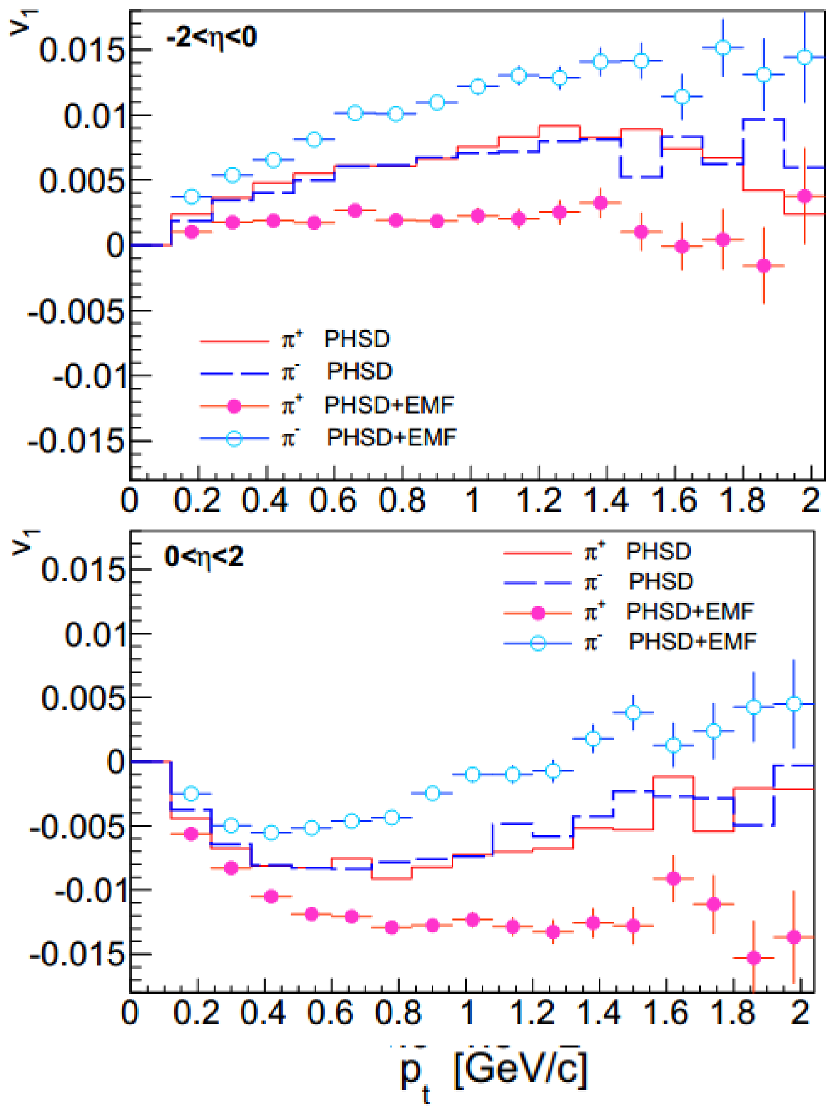

Distributions for the same hadron masses but opposite electric charges are splitted and this can be observed !

Charge-dependent v_1 distributions at NICA

Cu+Au (9 GeV)

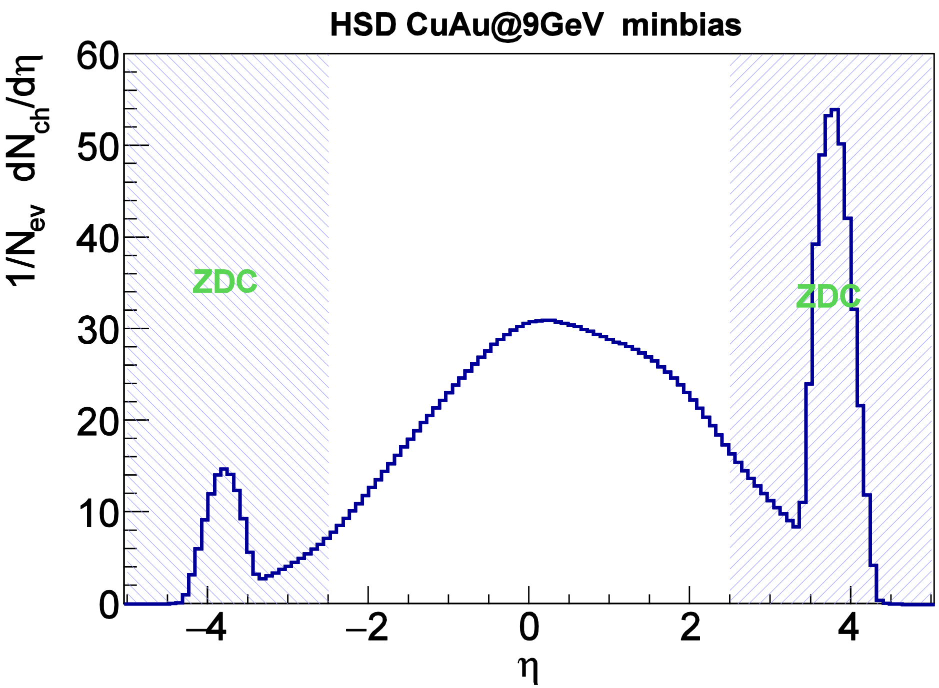

Charged pion v_1 disrtribution

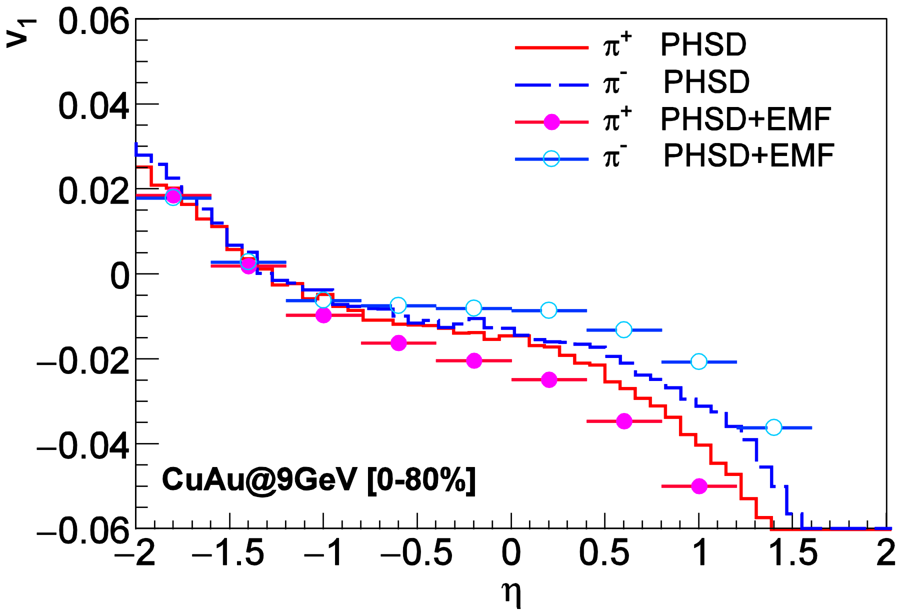

TPC: η<1.2 p_T>0.15 GeV/c

In the presence of the electromagnetic force the splitting of π^+ and π^- is clearly seen

Charge-dependent p_T distributions at NICA

The transverse momentum v_1 distributions of +/- pions are different in the Cu- and Au-sites. The shape of spectra differs in forward and backward semispheres

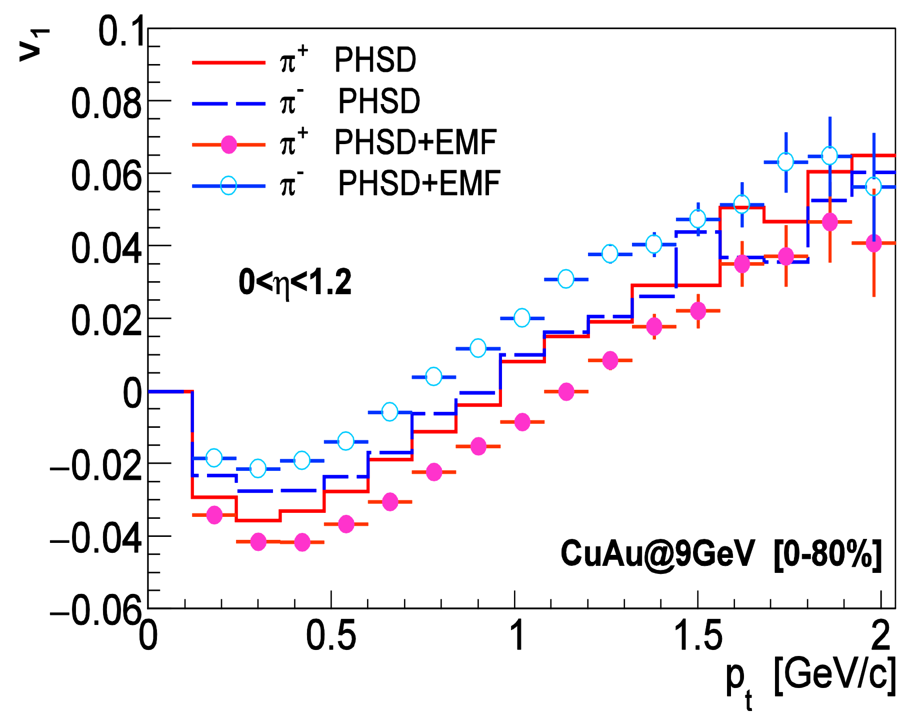

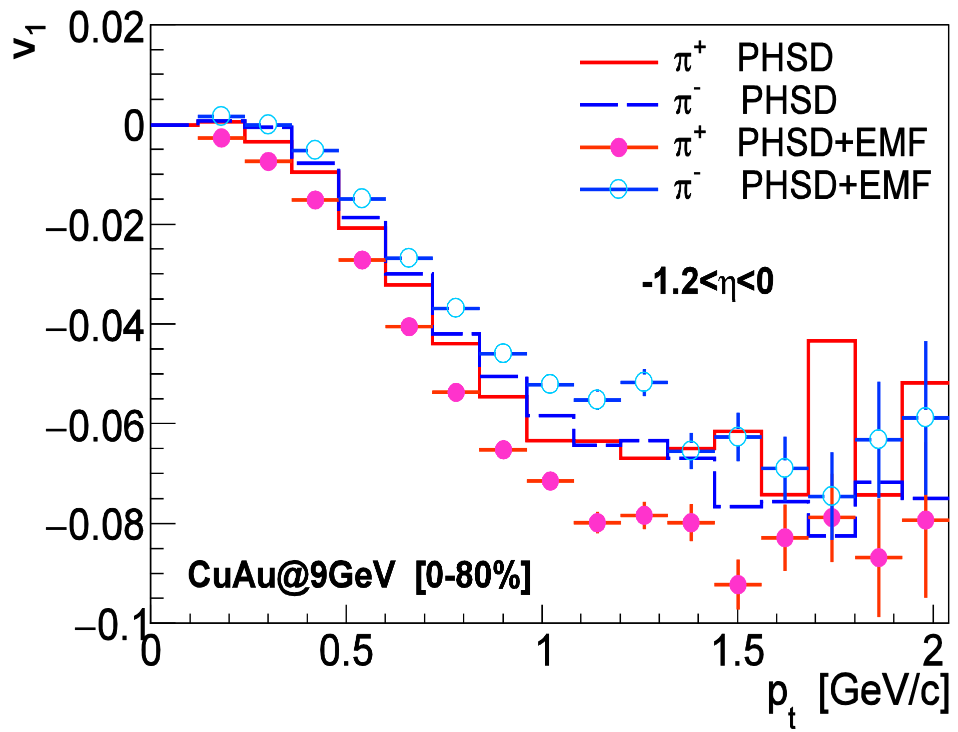

The difference between $v_1(p_T)$ for π^+ and π^- is prominent and getting larger with p_T increase

Protons-antiprotons

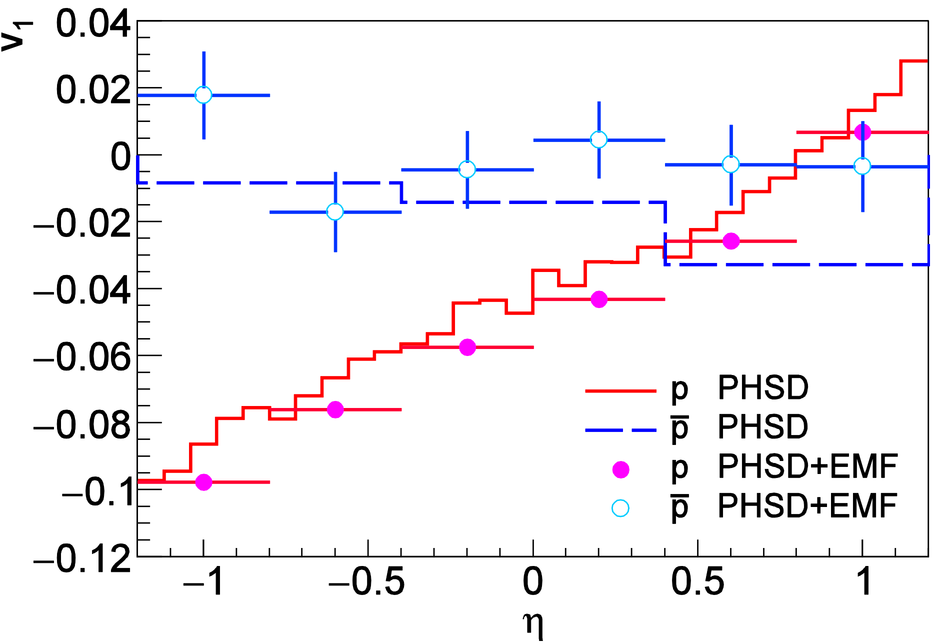

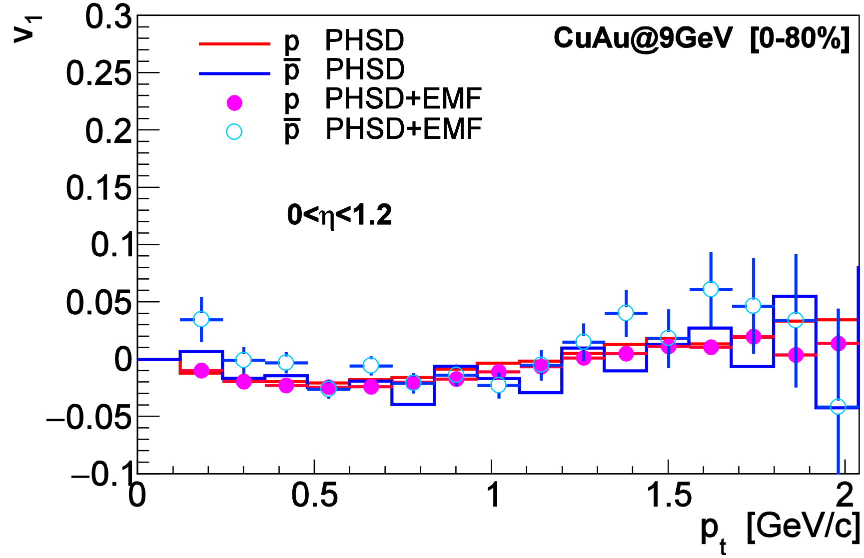

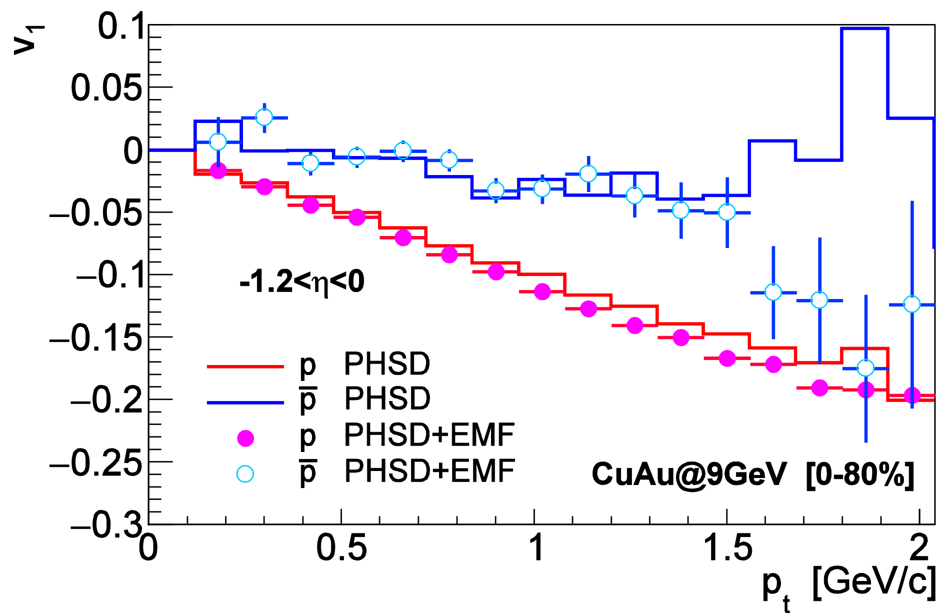

The η-spectra for protons and antiprotons are quite different (due to different reaction mechanisms) and weakly, if ever, influenced by electromagnetic effect.

Kaons-antikaons

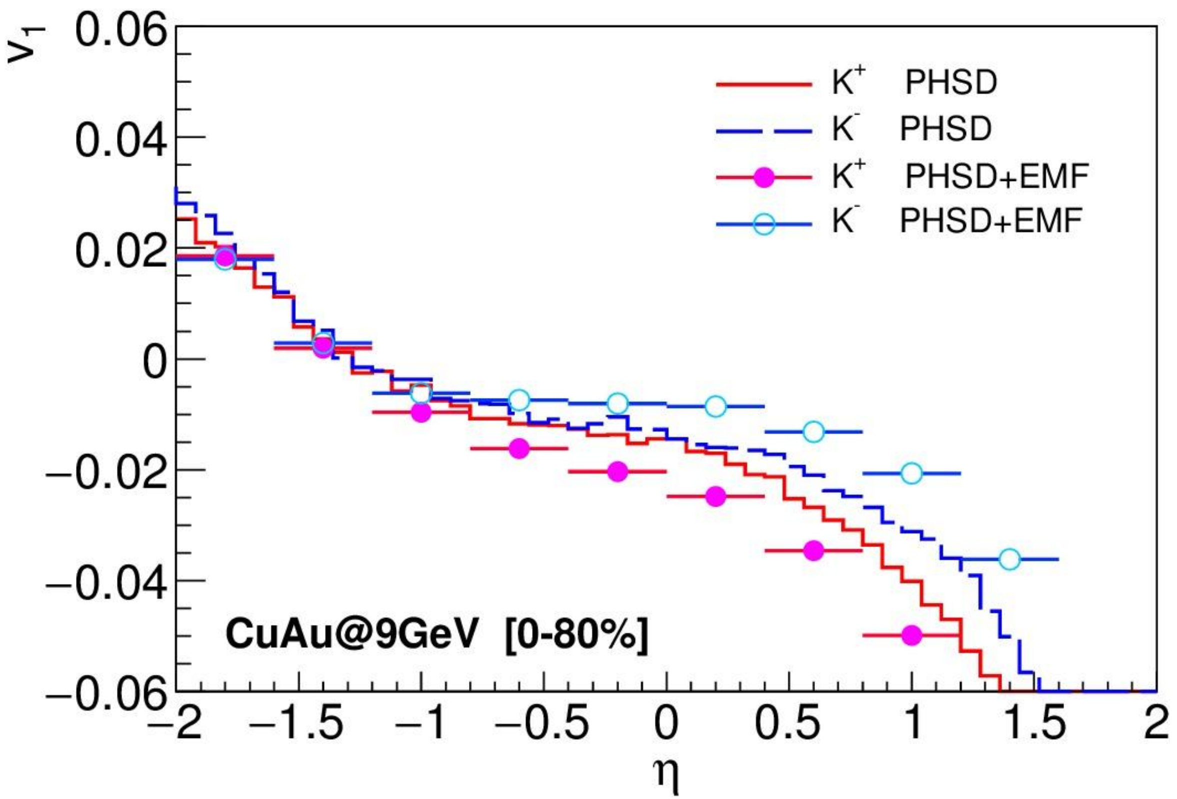

Distributions are very close to that for pions (but yields ?)

Summary

- The microscopic (Parton)-Hadron-String-Dynamics transport approach reproducing the general trend of observables for symmetric Au-Au collisions in a large energy range including the NICA energy is used and extended for creation of electromagnetic fields in relativistic heavy-ion collisions.

- It is demonstrated that for asymmetric systems – like Cu-Au ($\sqrt{s}$=9 GeV) collisions -- the directed flow is sensitive to inclusion of the electromagnetic field. Numerical estimates are given.

- Observation of splitting in charge-dependent characteristics of the directed flow would evidence the existence of strong electromagnetic fields created in the course of nuclear reaction.